

Structure–function relationship exploration for enhanced electro-optic activity in isophorone-based organic NLO chromophores



Fenggang Liu^{a,*}, Hua Zhang^b, Hongyan Xiao^b, Huajun Xu^b, Shuhui Bo^b, Ling Qiu^b, Zhen Zhen^b, Lijie Lai^a, Shujie Chen^a, Jiahai Wang^{a,**}

^a School of Chemistry and Chemical Engineering, Guangzhou Key Laboratory for Environmentally Functional Materials and Technology, Guangzhou University, Guangzhou 510006, PR China

^b Key Laboratory of Photochemical Conversion and Optoelectronic Materials, Technical Institute of Physics and Chemistry, Chinese Academy of Sciences, Beijing 100190, PR China

ARTICLE INFO

Keywords:

Nonlinear optics
Chromophore
Isolation group
Electro-optic
Isophorone
Structure–function

ABSTRACT

Four isophorone-based chromophores FLD1–FLD4 has been synthesized and investigated based on julolidinyl donors, with modified isophorone-derived bridges and tricyanovinyl-dihydrofuran or phenyl-trifluoromethyl-tricyanofuran acceptors. The chromophore FLD3 was modified with a 2-((tert-butyl-dimethylsilyloxy)ethanethiol group covalently attached to the π -conjugate bridge to ensure its all-trans conformation and prevent close packing of molecules, which benefit the macroscopic electro-optic efficiency. The chromophore FLD3 possesses better thermal stability than chromophore FLD1 without the isolation group on the bridge. Moreover, density functional theory calculations suggested that the hyperpolarizability (β) value of chromophore FLD3 is larger than that of chromophore FLD1. Polymers doped with chromophore FLD3 have been poled to afford ultrahigh electro-optic coefficient (r_{33}) of 238 pm/V at 1.31 μm , which is nearly 60% higher than that obtained from chromophore FLD1 and three times higher than that of analogue chromophores FLD2 and FLD4.

1. Introduction

With the development of the information technology, conventional microelectronic materials, usually using electrons as the carriers, will have difficulty satisfying the needs for future communication technology [1]. Compared with electronic communication, transmission of information by photonics has many advantages such as high frequency, wide bandwidth, high speed, and good parallelism [2,3]. The ability to convert signals between electronic and photonic domains is central to photonic/electronic integration. Materials and devices that effect such transduction are referred to as “electro-optic” (EO) [4]. The organic electro-optic (OEO) materials have attracted great attention in last thirty years. Compared with inorganic materials, OEO materials have potential advantages such as lower cost, ease of processing, larger EO coefficients and so on [5,6].

The second-order nonlinear optical (NLO) chromophores are the key constructing blocks for OEO materials [7–11]. To meet the stringent requirements for the using of devices, OEO materials should be developed through rational design of nonlinear optical (NLO) chromophores to optimize their first hyperpolarizability (β), and effectively translate

these large β values into bulk EO activities. Meanwhile, improvements of other auxiliary properties like high thermal and photochemical stability, good transparency, as well as easy syntheses are very important.

The second-order NLO chromophores are based on a push-pull system, which consists of an electron-donating group (Donor) and an electron-withdrawing group (Acceptor) coupled through a π -conjugated bridge which called (D– π –A) configuration [12]. The donor moiety has largely been of the amine structure [13]. Bridge moieties consisted of heteroaromatic (thiophene, pyrrole, furan) or polyene (phenyltetraene) structures have reported [14–17]. The acceptor moieties have developed from weaker nitro, cyano, alkoxy, isoxazolone, tricyanovinyl, diarylthiobarbituric acid groups to strong and effective tricyanovinyl-dihydrofuran (TCF) and phenyl-trifluoromethyl-tricyanofuran (CF₃-Ph-TCF) groups [1,13,18]. Among which, the CLD-type chromophores (containing the ring-locked tetraene bridges) with TCF or CF₃-Ph-TCF acceptor were widely investigated due to their large β and good utility for EO devices [19]. Relatively high electro-optic (EO) coefficients r_{33} around 40–70 pm/V measured at the wavelengths of 1.3 μm have been achieved from poled polymeric composites using these polyenic chromophores as dopants [20]. There remains strong

* Corresponding author.

** Corresponding author.

E-mail addresses: liufg6@gzhu.edu.cn (F. Liu), jiahaiwang@gzhu.edu.cn (J. Wang).

continued interest in improving the properties of these materials as well as the synthetic strategies for their preparation.

Julolidinyl-based group as the electron donor has been reported with better solubility, stronger electron-donating ability and larger steric hindrance than the classical dimethylanilino moiety [21]. The ring-fused aminophenyl structures in julolidinyl donors facilitate the overlap of the p-orbital of the amino atom with the phenyl ring thus providing a good mechanism to increase the electron-donating strength [22]. Meanwhile, the steric hindrance and tension of the rigid structure from the julolidinyl-based donor in chromophore can also suppress aggregations. So, the electro-optic coefficient of the chromophore can be further improved by using julolidinyl-based group as the donor. Previous study showed that the CLD-type chromophores are often a mixture of trans and cis isomers. The chromophore with cis and trans configuration showed reduced $\mu\beta$ value than that of chromophore with all-trans conformation. And attempts to purify these isomers through column chromatography for higher NLO activity are proven to be very difficult [20].

So, in this paper, we want to increase the electro-optic activity of isophorone-based chromophore furthermore. We use julolidinyl group as the donor of the chromophore. Meanwhile, we utilized epoxyisophorone ring-opening chemistry to efficiently incorporate the 2-((tert-butylidimethylsilyl)oxy)ethanethiol (STBDMS) group to the bridge of julolidinyl-based chromophores FLD3-FLD4 (Chart 1) to ensure its all-trans conformation. The modification of STBDMS group on the chromophore can prevent close packing of molecules, which in turn, may attenuate the strong dipole-dipole electrostatic interactions between chromophores to improve poling efficiency of EO polymers. And compared with the nonsubstituted analogue chromophore FLD1, thiolated chromophore FLD3 achieves higher molecular hyperpolarizability because of unique and moderate π -accepting ability of the substituted group. In the meantime, we synthesized chromophore FLD4 with the same donor and bridge but with a different CF_3 -Ph-TCF acceptor.

We compare the structure-property relationship between the 4-s order chromophores with julolidinyl-based donors and tetraene-derived bridge, but with different position and quantity of the functionalized connecting spacer and different acceptor. As shown in Chart 1, the chromophores FLD1 and FLD2 have only one side-group covalently attached to the donor. The chromophores FLD3 and FLD4 have one side-groups covalently attached to the donor and other one side-groups covalently attached to the π -system bridge. The four chromophores have similar D- π -A structure, but differ in the position and quantity of the spacer, allowing us to investigate the influence of the spacer on the poling-induced alignment of the chromophores. The UV-Vis, solvatochromic behavior, DFT quantum mechanical calculations, thermal stabilities and EO activities of these chromophores were systematically studied and compared to understand their structure-property relationships. An electro-optic (EO) coefficient of 238 pm/V at 1.31 μm was obtained for film FLD3/APC, which is nearly 60% higher than that obtained from analogue chromophore FLD1 and much higher than chromophore FLD2 and FLD4 as well as similar reported monolithic materials like chromophore CLD-1 [23] and chromophore YLD-124 [24].

2. Experimental

2.1. Materials and instrument

All chemicals are commercially available and are used without further purification unless otherwise stated. *N,N*-dimethylformamide (DMF) and tetrahydrofuran (THF) were distilled over calcium hydride and stored over molecular sieves (pore size 3 Å). Compounds 2b-6b and chromophores FLD1 and FLD2 were synthesized according to literature [25]. TLC analyses were carried out on 0.25 mm thick precoated silica plates and spots were visualized under UV light. Chromatography on silica gel was carried out on Kieselgel (200–300 mesh).

^1H NMR spectra were determined on an Advance Bruker 400 M (400 MHz) NMR spectrometer (tetramethylsilane as internal reference). The MS spectra were obtained on MALDI-TOF (Matrix Assisted Laser Desorption/Ionization of Flight) on BIFLEXIII (Broker Inc.,) spectrometer. The UV-Vis spectra were performed on Cary 5000 photo spectrometer. The TGA was determined by TA5000-2950TGA (TA co) with a heating rate of 10 $^\circ\text{C min}^{-1}$ under the protection of nitrogen.

2.2. Syntheses

2.2.1. Synthesis of 8-(2-((tert-butylidimethylsilyl)oxy)ethoxy)-1,1,7,7-tetramethyl-2,3,6,7-tetrahydro-1H,5H-pyrido[3,2,1-ij]quinoline-9-carbaldehyde (Compound 2a)

Under a N_2 atmosphere, anhydrous potassium carbonate (2.4 g, 15 mmol) was added to a solution of compound 1 (2.73 g, 10 mmol) and compound tert-butyl(2-chloroethoxy)dimethylsilane (2.92 g, 15 mmol) in DMF (90 mL). The mixture was allowed to stir at 90 $^\circ\text{C}$ for 12 h and then poured into water. The organic phase was extracted by AcOEt, washed with brine and dried over MgSO_4 . After removal of the solvent under reduced pressure, the crude product was purified by silica chromatography, eluting with (Acetone: Hexane = 1:10) to give compound 2a as a yellow powder with 90.7% yield (3.91 g, 9.07 mmol). MS (MALDI-TOF), m/z : 431.59 (M^+). ^1H NMR (300 MHz, CDCl_3) δ 9.98 (s, 1H), 7.58 (s, 1H), 4.06–3.99 (m, 4H), 3.32–3.26 (m, 2H), 3.25–3.20 (m, 2H), 1.74–1.57 (m, 4H), 1.44 (s, 6H), 1.26 (s, 6H), 0.91 (s, 9H), 0.11 (m, 6H). ^{13}C NMR (126 MHz, CDCl_3) δ 187.72, 161.44, 148.29, 126.10, 125.73, 120.91, 117.04, 79.10, 62.48, 47.49, 47.45, 46.86, 46.83, 39.38, 35.69, 32.56, 32.04, 29.87, 26.03, 25.90, 18.37, –5.12. Anal. Calcd (%) for $\text{C}_{25}\text{H}_{41}\text{NO}_3\text{Si}$: C, 69.56; H, 9.57; N, 3.24; found: C, 69.57; H, 9.55; N, 3.23;

2.2.2. Synthesis of (E)-3-(2-(8-(2-((tert-butylidimethylsilyl)oxy)ethoxy)-1,1,7,7-tetramethyl-2,3,6,7-tetrahydro-1H,5H-pyrido[3,2,1-ij]quinolin-9-yl)vinyl)-2-((2-((tert-butylidimethylsilyl)oxy)ethyl)thio)-5,5-dimethylcyclohex-2-en-1-one (Compound 3a)

To a solution of ethanol (30 mL) was carefully added sodium metal (0.23 g, 10.00 mmol) under N_2 atmosphere. The solution was vigorously stirred at room temperature until the sodium was completely dissolved. 1-Butanethiol (0.78 g, 10 mmol) was added to the above solution by syringe, and the mixture was stirred for 10 min followed by addition of isophoroneoxide (1.54 g, 10.00 mmol). The mixture became dark shortly and was stirred at room temperature for another 1 h to form intermediate. Compound 2a (2.16 g, 5.00 mmol) was added to the mixture which was then heated to 65 $^\circ\text{C}$ for 18 h. After the removal of solvent, the residue was directly purified by column chromatography on silica gel (hexane/ethyl acetate, v/v, 6/1) to afford a red solid 3a in 76.3% yield (2.40 g, 3.82 mmol). MS (MALDI-TOF), m/z : 628.03 (M^+). ^1H NMR (300 MHz, CDCl_3) δ 7.88 (d, $J = 16.2$ Hz, 1H), 7.39 (s, 1H), 7.34 (d, $J = 16.2$ Hz, 1H), 4.04 (t, $J = 5.1$ Hz, 2H), 3.90 (t, $J = 5.1$ Hz, 2H), 3.56 (m, 3H), 3.27–3.21 (m, 2H), 3.20–3.12 (m, 2H), 2.82 (t, $J = 5.2$ Hz, 2H), 2.65 (s, 2H), 2.44 (s, 2H), 1.75–1.69 (m, 4H), 1.43 (s, 6H), 1.29 (s, 6H), 1.07 (s, 6H), 0.91 (s, 9H), 0.13 (s, 6H). ^{13}C NMR (126 MHz, CDCl_3) δ 197.20, 161.16, 157.25, 144.72, 135.40, 126.94, 126.16, 123.62, 122.53, 122.21, 116.68, 76.33, 62.55, 60.27, 51.64, 47.41, 46.83, 41.47, 39.89, 38.78, 36.18, 32.71, 32.36, 32.22, 30.81, 30.12, 30.09, 28.45, 28.42, 26.06, 26.02, 18.48, –5.11. Anal. Calcd (%) for $\text{C}_{36}\text{H}_{55}\text{NO}_4\text{Si}$: C, 68.85; H, 9.15; N, 2.23; found: C, 68.83; H, 9.13; N, 2.24;

2.2.3. Synthesis of (E)-3-(2-(8-(2-((tert-butylidimethylsilyl)oxy)ethoxy)-1,1,7,7-tetramethyl-2,3,6,7-tetrahydro-1H,5H-pyrido[3,2,1-ij]quinolin-9-yl)vinyl)-2-((2-((tert-butylidimethylsilyl)oxy)ethyl)thio)-5,5-dimethylcyclohex-2-en-1-one (Compound 4a)

To a solution of compound 3a (1.88 g, 3.00 mmol) and imidazole (0.25 g, 3.60 mmol) in DMF (10 mL), tert-Butyldimethylsilyl chloride (0.55 g, 3.60 mmol) was slowly under N_2 at room temperature. After

vigorously stirring for 3 h, the reaction was quenched by being poured into 100 mL H₂O. The crude product was extracted with hexane (3 × 50 mL). The combined organic layer was washed with H₂O, dried (Na₂SO₄), filtered, and concentrated at reduced pressure. The crude product was purified by column chromatography using ethyl acetate and hexane (v/v, 1:10 to 1:5) as the eluent to afford a red solid 4a in 94.1% yield (2.10 g, 2.82 mmol). MS (MALDI-TOF), *m/z*: 742.23 (M⁺). ¹H NMR (300 MHz, CDCl₃) δ 7.83 (d, *J* = 16.2 Hz, 1H), 7.38 (s, 1H), 7.29–7.22 (d, *J* = 16.2 Hz, 1H), 4.02 (t, *J* = 5.1 Hz, 2H), 3.88 (t, *J* = 5.1 Hz, 2H), 3.73–3.66 (m, 2H), 3.23–3.18 (m, 2H), 3.15–3.11 (m, 2H), 2.87 (m, 2H), 2.61 (s, 2H), 2.40 (s, 2H), 1.73–1.67 (m, 4H), 1.43 (s, 6H), 1.28 (s, 6H), 1.06 (s, 6H), 0.92 (s, 9H), 0.83 (s, 9H), 0.12 (s, 6H), 0.01 (s, 6H). ¹³C NMR (126 MHz, CDCl₃) δ 195.67, 165.02, 156.95, 144.36, 133.83, 127.69, 126.89, 123.42, 123.19, 122.17, 117.06, 76.17, 63.31, 62.55, 52.01, 47.41, 46.83, 41.42, 39.99, 36.38, 35.82, 32.73, 32.48, 32.30, 32.22, 30.95, 30.67, 30.18, 28.44, 28.13, 26.03, 25.93, 18.52, 18.32, –5.11, –5.23. Anal. Calcd (%) for C₄₂H₇₁N₄O₄SSi₂: C, 67.96; H, 9.64; N, 1.89; found: C, 67.97; H, 9.63; N, 1.90;

2.2.4. Synthesis of (E)-2-(3-((E)-2-(8-(2-((tert-butylidimethylsilyl)oxy)ethoxy)-1,1,7,7-tetramethyl-2,3,6,7-tetrahydro-1H,5H-pyrido[3,2,1-ij]quinolin-9-yl)vinyl)-2-((2-((tert-butylidimethylsilyl)oxy)ethyl)thio)-5,5-dimethylcyclohex-2-en-1-ylidene)acetonitrile (Compound 5a)

A three-necked flask was charged with NaH (0.27 g, 11.2 mmol) in dry THF (12 mL) under N₂. Diethyl(cyanomethyl)phosphonate (1.81 mL, 1.99 g, 11.2 mmol) was slowly introduced to the mixture dropwise by syringe. After the solution became clear, compound 4a (1.68 g, 2.25 mmol) in THF (5 mL) was added to the mixture which was directly refluxed for 24 h. After the removal of THF in vacuo, the residue was directly purified by the column chromatography on silica gel using ethyl acetate and hexane (v/v, 1:8 to 1:6) as the eluent to afford a red solid 5a in 73.1% yield (1.26 g, 1.64 mmol). MS (MALDI-TOF), *m/z*: 765.26 (M⁺). ¹H NMR (500 MHz, CDCl₃) δ 7.83 (d, *J* = 16.2 Hz, 1H), 7.39 (s, 1H), 7.16 (d, *J* = 16.2 Hz, 1H), 6.29 (s, 1H), 4.06 (t, *J* = 4.8 Hz, 2H), 3.94 (t, *J* = 4.8 Hz, 2H), 3.73 (t, *J* = 5.6 Hz, 2H), 3.25 (t, *J* = 4.8 Hz, 2H), 3.17 (d, *J* = 4.8 Hz, 2H), 2.74 (m, 2H), 2.62 (s, 2H), 2.52 (s, 2H), 1.76 (m, 4H), 1.47 (s, 6H), 1.34 (s, 6H), 1.06 (s, 6H), 0.98 (s, 9H), 0.90 (s, 9H), 0.17 (s, 6H), 0.06 (s, 6H). ¹³C NMR (126 MHz, CDCl₃) δ 158.58, 156.51, 149.42, 143.90, 131.51, 126.85, 125.67, 123.95, 123.17, 122.22, 119.22, 117.55, 94.30, 75.95, 62.65, 47.41, 46.81, 43.38, 41.76, 40.14, 37.69, 36.53, 32.74, 32.24, 31.08, 30.84, 30.22, 30.17, 29.71, 28.09, 26.04, 25.90, 18.50, 18.27, 14.14, 10.96, –5.11, –5.25. Anal. Calcd (%) for C₄₄H₇₂N₂O₃SSi₂: C, 69.06; H, 9.48; N, 3.66; found: C, 69.07; H, 9.47; N, 3.65;

2.2.5. Synthesis of (E)-2-(3-((E)-2-(8-(2-((tert-butylidimethylsilyl)oxy)ethoxy)-1,1,7,7-tetramethyl-2,3,6,7-tetrahydro-1H,5H-pyrido[3,2,1-ij]quinolin-9-yl)vinyl)-2-((2-((tert-butylidimethylsilyl)oxy)ethyl)thio)-5,5-dimethylcyclohex-2-en-1-ylidene)acetaldehyde (Compound 6a)

The solution of compound 5a (0.77 g, 1.00 mmol) in 20.0 mL of fresh dried toluene was cooled to –78 °C and the solution of Diisobutylaluminum hydride in hexanes (1.5 M, 2.72 mL, 4.00 mmol) was added dropwise. After being kept at –78 °C for 2 h, wet silica gel (1.2 g) with 10.0 mL of H₂O was added and the reaction mixture was stirred at 0 °C for 1 h. The organic products were extracted in ethyl acetate, washed with H₂O, and the solvent evaporated in vacuum. The residue was purified by the column chromatography on silica gel using ethyl acetate and hexane (v/v, 1:2 to 1:1) as the eluent to afford a red solid 6a in 71.1% yield (0.55 g, 0.71 mmol). MS (MALDI-TOF), *m/z*: 768.31 (M⁺). ¹H NMR (300 MHz, CDCl₃) δ 10.15 (d, *J* = 8.1 Hz, 1H, CHO), 7.90 (d, *J* = 16.2 Hz, 1H, CH), 7.37 (s, 1H, ArH), 7.13 (d, *J* = 16.2 Hz, 1H), 7.01 (d, *J* = 8.1 Hz, 1H), 4.03 (t, *J* = 5.0 Hz, 2H), 3.90 (t, *J* = 5.0 Hz, 2H), 3.73–3.67 (m, 2H), 3.24–3.18 (m, 2H), 3.17–3.12 (m, 2H), 2.76–2.70 (m, 2H), 2.76 (s, 2H), 2.51 (s, 2H), 1.77–1.70 (m, 4H), 1.44 (s, 6H), 1.31 (s, 6H), 1.26 (s, 6H), 1.03 (s, 6H),

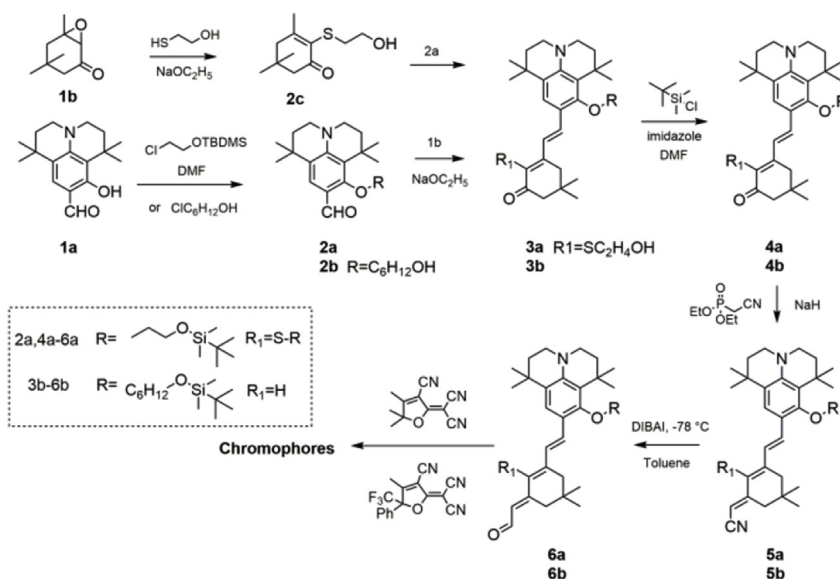
0.94 (s, 12H), 0.84 (s, 12H). ¹³C NMR (126 MHz, CDCl₃) δ 191.49, 156.70, 156.44, 150.45, 143.91, 131.35, 127.98, 126.86, 126.73, 124.66, 123.20, 122.26, 117.67, 75.91, 62.95, 62.56, 47.42, 46.88, 41.78, 40.12, 40.01, 37.41, 36.51, 32.75, 32.26, 31.08, 30.25, 30.07, 29.70, 28.37, 26.03, 25.89, 22.69, 18.52, 18.26, 14.13, –5.11, –5.24. Anal. Calcd (%) for C₄₄H₇₃N₄O₄SSi₂: C, 68.79; H, 9.58; N, 1.82; found: C, 68.77; H, 9.59; N, 1.81;

2.2.6. Synthesis of 2-(4-((1E,3E)-3-(3-((E)-2-(8-(2-((tert-butylidimethylsilyl)oxy)ethoxy)-1,1,7,7-tetramethyl-2,3,6,7-tetrahydro-1H,5H-pyrido[3,2,1-ij]quinolin-9-yl)vinyl)-2-((2-((tert-butylidimethylsilyl)oxy)ethyl)thio)-5,5-dimethylcyclohex-2-en-1-ylidene)prop-1-en-1-yl)-3-cyano-5,5-dimethylfuran-2(5H)-ylidene)malononitrile (Chromophore FLD3)

To a solution of 6a (0.31 g, 0.40 mmol) and the TCF acceptor (0.96 g, 0.48 mmol) in MeOH (60 ml) was added several drops of triethyl amine. The reaction was allowed to stir at 78 °C for 5 h. The reaction mixture was cooled and green crystal precipitation was facilitated. After removal of the solvent under reduced pressure, the crude product was purified by silica chromatography, eluting with (AcOEt: Hexane = 1:5) to give chromophore FLD3 as a green solid in 43.6% yield (0.17 g, 0.17 mmol). MS (MALDI-TOF), *m/z*: 949.43 (M⁺). ¹H NMR (400 MHz, CDCl₃) δ 8.14 (dd, *J* = 14.5, 12.5 Hz, 1H), 7.97 (d, *J* = 16.0 Hz, 1H), 7.53 (d, *J* = 12.2 Hz, 1H), 7.41 (s, 1H), 7.26 (s, 1H), 6.38 (d, *J* = 14.7 Hz, 1H), 4.04 (t, *J* = 5.2 Hz, 2H), 3.91 (t, *J* = 5.1 Hz, 2H), 3.73 (t, *J* = 7.2 Hz, 2H), 3.27 (t, *J* = 5.9 Hz, 2H), 3.23–3.16 (m, 2H), 2.74 (t, *J* = 7.2 Hz, 2H), 2.55 (m, 2H), 2.51 (m, 2H), 1.74 (d, *J* = 5.5 Hz, 4H), 1.70 (s, 6H), 1.45 (s, 6H), 1.32 (s, 6H), 1.03 (s, 6H), 0.94 (s, 8H), 0.86 (s, 10H), 0.14 (s, 6H), 0.02 (s, 6H). ¹³C NMR (101 MHz, CDCl₃) δ 176.25, 173.16, 157.11, 154.98, 152.51, 144.82, 144.47, 133.01, 129.39, 127.63, 126.96, 124.29, 123.23, 122.39, 117.65, 116.20, 112.63, 112.07, 111.75, 96.75, 93.65, 62.67, 62.45, 54.90, 47.44, 46.88, 41.76, 41.20, 39.75, 38.01, 36.11, 32.66, 32.16, 30.73, 30.27, 29.99, 28.30, 26.36, 25.96, 25.85, 18.44, 18.26, 0.95, –5.18, –5.25. Anal. Calcd (%) for C₅₅H₈₀N₄O₄SSi₂: C, 69.57; H, 8.49; N, 5.90; found: C, 69.59; H, 8.48; N, 5.91;

2.2.7. Synthesis of 2-(4-((1E,3E)-3-(3-((E)-2-(8-(2-((tert-butylidimethylsilyl)oxy)ethoxy)-1,1,7,7-tetramethyl-2,3,6,7-tetrahydro-1H,5H-pyrido[3,2,1-ij]quinolin-9-yl)vinyl)-2-((2-((tert-butylidimethylsilyl)oxy)ethyl)thio)-5,5-dimethylcyclohex-2-en-1-ylidene)prop-1-en-1-yl)-3-cyano-5-phenyl-5-(trifluoromethyl)furan-2(5H)-ylidene)malononitrile (Chromophore FLD4)

Compound 6a (0.31 g, 0.40 mmol) and CF₃-Ph-TCF acceptor (0.15 g, 0.48 mmol) were mixed with anhydrous ethanol (5 mL). The mixture was allowed to stir at 65 °C for 2 h. The solvent was removed under vacuum and the residual mixture was purified by flash chromatography on silica gel using ethyl acetate and hexane (v/v, 1: 4) to give chromophore FLD4 as a deep green solid in 73.2% yield (0.31 g, 0.29 mmol). MS (MALDI-TOF), *m/z*: 1065.51 (M⁺). ¹H NMR (300 MHz, Acetone) δ 8.14 (d, *J* = 15.1 Hz, 1H), 7.99 (s, 1H), 7.76–7.70 (m, 2H), 7.62 (m, 3H), 7.59 (d, *J* = 7.6 Hz, 2H), 7.51–7.33 (m, 1H), 6.53 (d, *J* = 15.1 Hz, 1H), 4.13 (t, *J* = 4.7 Hz, 2H), 3.99 (t, *J* = 4.7 Hz, 2H), 3.74 (t, *J* = 6.8 Hz, 2H), 3.51 (t, *J* = 5.9 Hz, 2H), 3.46–3.41 (m, 2H), 2.76 (t, *J* = 6.8 Hz, 2H), 2.71–2.22 (m, 4H), 1.81–1.74 (m, 4H), 1.47 (s, 6H), 1.32 (s, 6H), 0.96 (s, 15H), 0.84 (s, 9H), 0.17 (s, 6H), 0.01 (s, 6H). ¹³C NMR (126 MHz, Acetone) δ 175.87, 159.36, 158.05, 157.77, 156.84, 148.41, 144.35, 137.71, 131.50, 130.95, 129.98, 129.59, 128.78, 128.53, 126.78, 124.97, 124.18, 123.23, 121.65, 118.98, 116.65, 114.88, 112.84, 112.73, 112.24, 94.66, 94.42, 77.15, 62.46, 62.39, 51.83, 47.87, 47.19, 41.26, 41.08, 40.72, 38.94, 38.18, 35.15, 32.93, 32.52, 31.94, 30.41, 30.20, 29.75, 27.90, 27.19, 25.58, 25.43, 18.20, 17.98, –5.12, –5.23. Anal. Calcd (%) for C₆₀H₇₉F₃N₄O₄SSi₂: C, 67.63; H, 7.47; N, 5.26; found: C, 67.61; H, 7.48; N, 5.25;



Scheme 1. Synthetic routes for chromophores FLD1-FLD4.

3. Results and discussion

3.1. Synthesis and characterization

The synthesis of chromophores FLD1-FLD4 is depicted in Scheme 1. Starting from the julolidine donor intermediate compounds 1a, chromophores FLD1-FLD4 were synthesized in good overall yields through simple six step reactions: the free hydroxyl group on the julolidine donor was protected by the bulky tert-butyldimethylsilyl (TBDMS) group to protect the hydroxyl group, improve the solubility and provide a suitable isolation. In the presence of sodium ethoxide as the base, 2-mercaptoethanol can be easily deprotonated to form a nucleophilic thiolate which underwent ring-opening reaction of epoxyisophorone 1b to selectively generate 2-mercaptoethanol-substituted isophorone 2c. This intermediate can be reacted directly with compound 2a in one-pot via the Knoevenagel condensation to furnish compound 3a with a high overall yield. The hydroxyl group of compound 3a or 3b was protected by TBDMS group to afford compound 4a or 4b. By using the Wittig-Horner reaction, compound 4a or 4b was reacted with diethyl(cyanomethyl)phosphonate to result in trienenitrile 5a or 5b. The reduction with DIBAL-H followed by hydrolysis converted the nitrile group on 5a or 5b into the corresponding aldehyde 6a or 6b. The aldehyde-containing donor-bridge 6a or 6b was condensed with TCF or $\text{CF}_3\text{-Ph-TCF}$ acceptor to furnish the chromophore FLD1-FLD4 as green solids. All of the chromophores were fully characterized by mass spectra, $^1\text{H NMR}$, $^{13}\text{C NMR}$ and elemental analysis. These chromophores possess good solubility in common organic solvents, such as dichloromethane, chloromethane and acetone.

Compound 6b was cis- and trans-isomer mixtures as shown in Fig. 1, so the derived chromophores FLD1 and FLD2 were also mixtures with cis and trans conformation. The alkylation sterically rigidified the polyenic bridge to ensure its all-trans. So the compound 6a, possess all-trans conformation (Fig. 1). Compound 6a was condensed with the acceptor to afford the all-trans chromophores FLD3 and FLD4. Its all-trans conformation could provide a better conjugation and increase the $\mu\beta$ value of the chromophores significantly.

3.2. Thermal stability

The thermal stability of the chromophores was investigated using thermogravimetric analysis (TGA) as shown in Fig. 2 and Table 1. All the chromophores exhibited good thermal stabilities with the

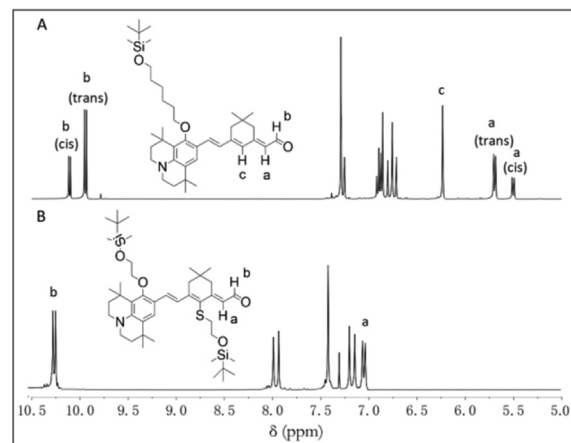


Fig. 1. $^1\text{H NMR}$ spectra of all-trans aldehyde 6a (B) in comparison with cis- and trans-isomer mixtures of aldehyde 6b (A).

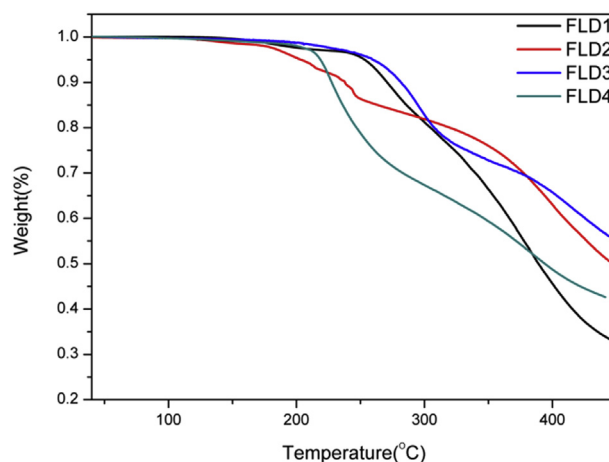


Fig. 2. TGA curves of chromophores FLD1-FLD4 with a heating rate of $10\text{ }^\circ\text{C min}^{-1}$ in nitrogen atmosphere.

decomposition temperatures (T_d) higher than $200\text{ }^\circ\text{C}$ ($202\text{ }^\circ\text{C}$ - $260\text{ }^\circ\text{C}$). Chromophore FLD3 has the highest decomposition temperature ($260\text{ }^\circ\text{C}$), followed by FLD1 ($253\text{ }^\circ\text{C}$), FLD4 ($219\text{ }^\circ\text{C}$) and FLD2 ($202\text{ }^\circ\text{C}$).

Table 1
Thermal and optical properties data of the chromophores.

Cmpd	T _d (°C)	λ _{max} ^a (nm)	λ _{max} ^b (nm)	Δλ ^c (nm)
FLD1	253	744	656	88
FLD2	202	975	771	204
FLD3	260	750	665	85
FLD4	219	961	753	208

λ_{max}^a was measured in chloroform. λ_{max}^b was measured in dioxane.
Δλ^c was the difference between λ_{max}^a and λ_{max}^b.

The T_d of chromophore FLD1 and FLD3 were higher than their analogues chromophores FLD2 and FLD4 with CF₃-Ph-TCF acceptor which is easy to understand because the TCF acceptor displays greater thermal stability than the analogues CF₃-Ph-TCF acceptor [26,27]. The T_d of chromophore FLD3 and FLD4 which contains a solubilizing STBDMS group at the bridge end were higher than their analogues chromophore FLD1 and FLD2. All the thermal stabilities of four chromophores were high enough for the application in EO device preparation [28].

3.3. Optical properties

We evaluated the UV–Vis absorption spectra of chromophores FLD1–FLD4 in various solvents with different dielectric constants as shown in Figs. 3 and 4. The spectral data are summarized in Table 1. The absorption maxima (λ_{max}) of FLD1 and FLD3 are located at 656 nm and 665 nm in dioxane and 744 nm and 750 nm in chloroform, respectively (Table 1). The λ_{max} of chromophore FLD3 with STBDMS substituted at the bridge are all bathochromically shifted (6–9 nm) compared to those of the corresponding unsubstituted analogue chromophore FLD1. These spectral characteristics can be rationalized by the fact that without a huge strong end-capped acceptor to pull electron, the neutral form will prevail over the charge separated form in the ground state. Therefore, these intermediates show a higher degree of BLA [29]. As a result, the STBDMS substitution in these systems simply acts as a weak acceptor and results in decreased band gap. However, when coupled with a strong CF₃-Ph-TCF acceptor, the degree of BLA of highly polarized push-pull chromophore FLD2 and FLD4 is reduced, in comparison with chromophore FLD2, chromophore FLD4 exhibited blue-shifted maximum absorptions, for example, the λ_{max} of chromophore FLD4 was 14 nm shorter than that of its analogue chromophore FLD2 in chloroform.

Besides, the solvatochromic behavior was also an important aspect to investigate the polarity of chromophores. As shown in Fig. 4, in non-polar solvents such as dioxane and toluene, all four chromophores exhibited a similar broad π–π* intramolecular charge-transfer (ICT) absorption band. However, in more polar solvents including chloroform,

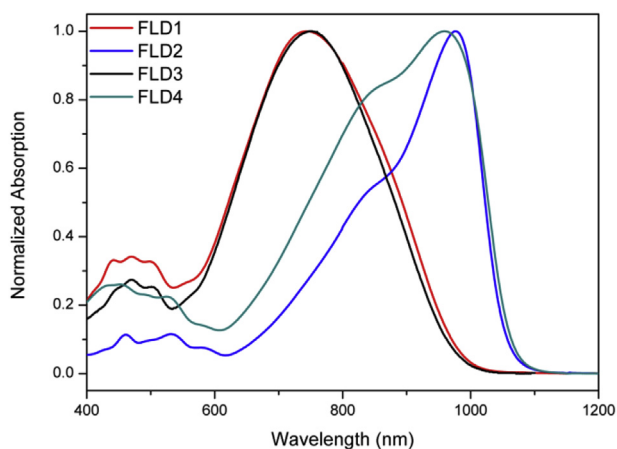


Fig. 3. UV–Vis absorption spectra of chromophores FLD1–FLD4 in chloroform.

acetone and acetonitrile, chromophores FLD1–FLD4 showed remarkably distinct optical features in solvatochromism and absorption band shape. With the solvents varying from the dioxane to the chloroform, a continuous shift of the absorption maxima to longer wavelength was observed for all the four chromophores. More dramatic effects were observed while investigating the absorption spectra of the four chromophores in highly polar solvents, such as chloroform, acetone and acetonitrile. Chromophores FLD1 and FLD3 showed a bathochromic shift of its absorption maximum initially and reversed to a hypsochromic shift for more polar solvents of acetone and acetonitrile, namely inverted solvatochromism [30]. However, a saturation behavior was found for chromophores FLD2 and FLD4 in the more polar solvents, such as acetone and acetonitrile. The absorption peak of chromophores FLD2 and FLD4 in these solvents exhibited almost no shift with increase of solvent polarity. It was accompanied by a noticeable spectral shape change showing a dominant low-energy absorption peak and a high-energy shoulder. The chromophores FLD2 and FLD4 showed a sharp and intense cyanine-type absorption band with a dramatically narrowed bandwidth in highly polar solvents. These interesting solvent-dependent spectral behaviors of chromophores FLD2 and FLD4 suggested that the more dipolar chromophore FLD2 and FLD4 can be polarized quite close to the cyanine limit, or even beyond that into the zwitter-ionic regime in the most polar solvents [31].

3.4. Theoretical calculations

To understand the ground-state polarization and microscopic NLO properties of the designed chromophores, the DFT calculations were carried out at the B3LYP level by employing the split valence 6-31G basis set using the Gaussian 09 program package [32]. The first hyperpolarizability (β) were carried out at the cam-B3LYP level by employing the split valence 6-31G basis set using the Gaussian 09 program package [33]. All molecules were assumed to be in trans-configurations [34]. The HOMO-LUMO energy gap, dipole moment (μ), β and μβ of the chromophores obtained from DFT calculations are summarized in Table 2.

The HOMO-LUMO energy gap was used to understand the charge transfer interaction occurring in a chromophore molecule [35]. Fig. 5 depicts the electron density distribution of the HOMO and LUMO structures. It can be seen that the density of the ground and excited state electron is asymmetry along the dipolar axis of the chromophores. The HOMO-LUMO energy gaps ΔE (DFT) were calculated by DFT calculations as shown in Table 2. The energy gaps between the HOMO and LUMO energy for chromophores FLD1–FLD4 were 1.933 eV, 1.859 eV, 1.923 eV and 1.863 eV, respectively. As ΔE is reduced, resulting in a bathochromic shift of λ_{max} within the series of compounds. These results correspond with the conclusion of UV–Vis spectra analysis.

The HOMO-LUMO energy gap is used to understand the charge transfer interaction that occurs within a molecular, In many cases, not only HOMO and LUMO states, the transitions related with HOMO-1, -2 and LUMO +1, +2 states are strongly contributed in such long conjugated materials [36]. So, the combined molecular orbital energy level graph constituted by LUMO +2 to HOMO-2 for all the four chromophores is given in Fig. 6.

The geometrically optimized structures of the molecules were investigated by calculating the dihedral angles of the donor moieties as shown in Fig. 7. For example, in chromophore FLD1, the silane chain substituent located on the oxygen atom of the donor made a large dihedral angle of 73.02° with average plane of the chromophore. As for chromophore FLD3, the silane chain substituent located on the donor and the bridge made a dihedral angle of 71.12° and 76.39° with average plane of the chromophore, respectively. These large dihedral angles caused large steric hindrance that suppressed aggregations among molecules.

As reported earlier, the β value has a close relationship with the strength of the donor and acceptor end groups and on the nature and

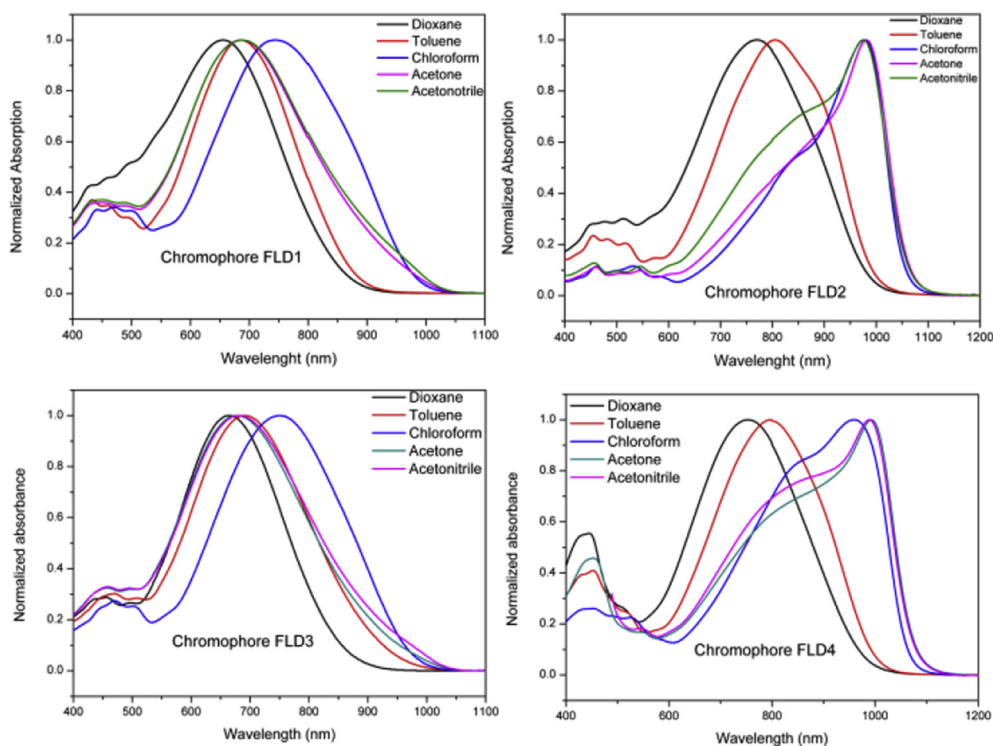


Fig. 4. UV-Vis absorption spectra of chromophores FLD1-FLD4 in five kinds of aprotic solvents with varying dielectric constants.

Table 2

Summary of DFT and EO coefficients of the chromophores.

Cmpd	$\Delta E(\text{DFT})^a$ (eV)	β_{tot}^b (10^{-30} esu)	μ^c (D)	$\mu\beta$ (10^{-48} esu)	r_{33} (pm/V)
FLD1	1.933	966.6	24.86	24029.6	150
FLD2	1.859	1137.8	25.36	28854.6	58
FLD3	1.923	1039.6	25.02	26010.8	238
FLD4	1.863	1186.6	26.12	30993.9	82

$\Delta E(\text{DFT})^a$ was calculated from DFT calculations.

β_{tot}^b is the first-order hyperpolarizability calculated from DFT calculations.

μ^c is the total dipole moment.

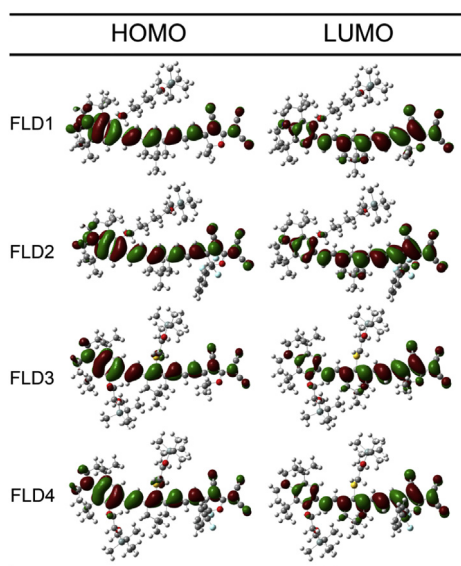


Fig. 5. Frontier molecular orbitals HOMO and LUMO of chromophores FLD1-FLD4.

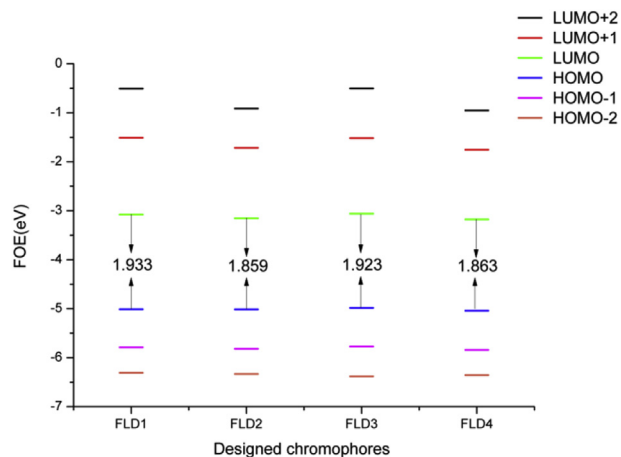


Fig. 6. Molecular orbital energy level diagram of chromophores FLD1-FLD4.

length of the bridge, substituents, steric hindrance and intramolecular charge-transfer and so on [35]. The β value of chromophore FLD2 and FLD4 were larger than that of chromophore FLD1 and FLD3 due to narrower energy gap between HOMO and LUMO, illustrating that the increased acceptor strength of the chromophores significantly increase their microscopic hyperpolarizability. Chromophore FLD3 exhibited a larger β value compared to that of chromophore FLD1, This shows that the perturbation of STBDMS substituent does not affect the efficient one-dimensional charge-transfer excitation which determines the principal tensor within a two-level model [37]. Instead, an auxiliary π -accepting STBDMS group conjugated with the amino donor and located in the middle of the bridge may potentially generate a small off-diagonal component of the two-dimensional tensor [38]. The enhanced value of chromophore FLD3 might be ascribed to the unique and moderate π -accepting ability of the substituted group STBDMS.

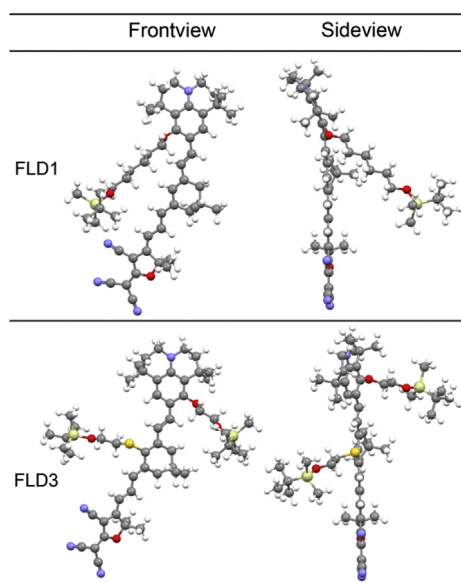


Fig. 7. Optimized structures of chromophores FLD1–FLD4.

3.5. Electro-optic performance

In order to investigate the translation of the microscopic hyperpolarizability into macroscopic EO response, the polymer films doped with different doping concentration of chromophores into amorphous polycarbonate (APC) were prepared using dibromomethane as solvent. The resulting solutions were filtered through a 0.2- μm PTFE filter and spin-coated onto indium tin oxide (ITO) glass substrates. Films of doped polymers were baked at 80 °C in a vacuum oven overnight. The corona poling process was carried out at a temperature of 10 °C above the glass transition temperature (T_g) of the polymer. The r_{33} values of poled films were measured by Teng-Man simple reflection method at a wavelength of 1310 nm using carefully selected thin ITO electrode with low reflectivity and good transparency in order to minimize the contribution from multiple reflections [39].

The measured r_{33} values depend on the chromophore number density (N), β value, and poling efficiency, described by the $\cos^3(\theta)$ order parameter, as indicated by Ref. [40].

$$r_{33} \approx |2N\beta f \langle \cos^3 \theta \rangle / n^4| \quad (1)$$

Where the f term describes electric-field factors and n is the refractive index of the film, both of which remain relatively constant for related chromophores at similar loading densities. $\cos^3(\theta)$ is the acentric order parameter. θ is the angle between the permanent dipole moment of chromophores and the applied electric field. At low concentration, the electro-optic activity increased with chromophore density, dipole moment and the strength of electric poling field. However, when the concentrations of chromophores increased to a certain extent, the N and $\cos^3(\theta)$ are no longer independent factor. Then,

$$\langle \cos^3(\theta) \rangle = (\mu F / 5kT) [1 - L^2(W/kT)] \quad (2)$$

Where k is the Boltzmann constant and T is the Kelvin (poling) temperature. $F = [f(0) E_p]$ where E_p is the electric poling field. L is the Langevin function, which is a function of W/kT , the ratio of intermolecular electrostatic energy (W) to the thermal energy (kT). L is related to electrostatic interactions between molecules.

This relationship succeeds in qualitatively predicting the important trends involving electro-optic activity although not the quantitative values of electro-optic coefficients. When the intermolecular electrostatic interactions are neglected, the electro-optic coefficient (r_{33}) should increase linearly with chromophore density, dipole moment, first hyperpolarizability and the strength of electric poling field. But

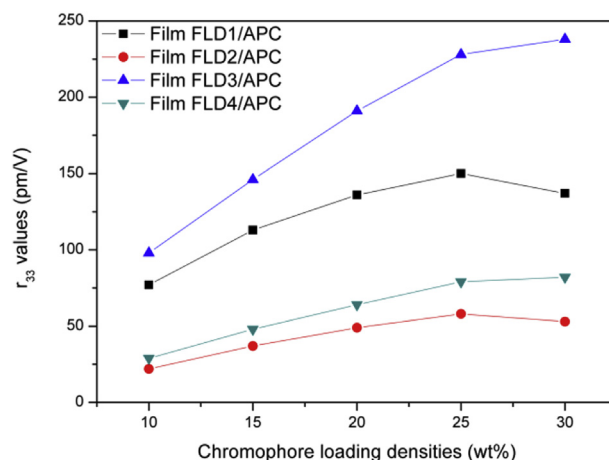


Fig. 8. r_{33} values of NLO thin films as a function of chromophore loading densities.

chromophores with large dipole moment generate intermolecular static electric field dipole-dipole interaction, which leads to the unfavorable antiparallel packing of chromophores. So the number of truly oriented chromophore (N) is small. In molecular optimization, introducing the huge steric hindrance group to isolate chromophores is the most popular and easy way to attenuate the dipole-dipole interactions of chromophores [41].

To evaluate their EO activities, 10 wt% of the chromophores FLD1–FLD4 were doped into APC and formulated as the typical guest–host polymer. By avoiding severe intermolecular electrostatic interactions at this modest number density of chromophores, the EO performance of thin film materials could be viewed as being more related to the intrinsic molecular properties for a deeper understanding of the structure–property relationships within this series of chromophore [42].

The E-O coefficients obtained from the optimal poling conditions are summarized in Fig. 8. For this series of chromophores, the poled films of FLD1/APC, FLD2/APC, FLD3/APC and FLD4/APC afforded r_{33} values of 77, 22, 98 and 29 pm/V, respectively. The film-FLD3/APC achieved the largest r_{33} value probably due to its large β and good polarizability. With relative lower β , the r_{33} value of film-FLD1/APC was smaller than that of film-FLD3/APC. The dramatic drop in EO activity from FLD1/APC to FLD2/APC and FLD3/APC to FLD4/APC is mainly associated with the inefficient poling due to its relatively high conductivity under the poling conditions. The absorption maxima (λ_{max}) of chromophore FLD2 and chromophore FLD4 are located at

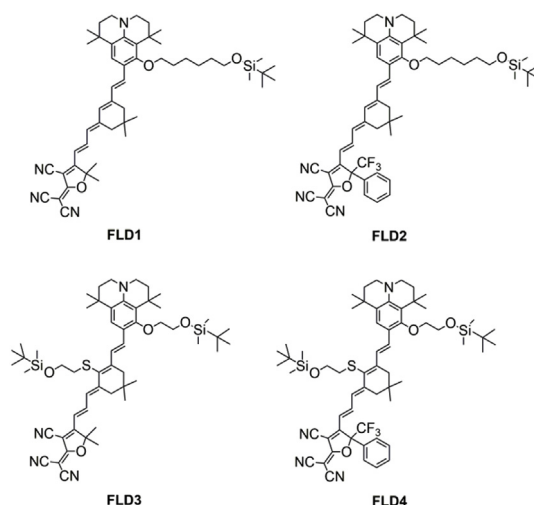


Chart 1. Chemical structure for chromophores FLD1–FLD4.

982 nm and 993 nm in acetone. The intramolecular electron transfer is very strong which was related to the stronger ICT ability, made it more sensitive to the ambient environment and thus lead to the relatively poor photostability and chemical stability. Such a subtle difference in the structure of the acceptor between CF₃-Ph-TCF and TCF could change the EO property of chromophores in a large degree. Chromophores with stronger CF₃-Ph-TCF acceptor were reported showing larger NLO properties than chromophores with normal TCF acceptor [43]. However, in this study, relatively weak TCF acceptor could profoundly improve the macroscopic nonlinearities for chromophore FLD1 and FLD3 with julolidinyl-based donor and tetraene-derived bridge. So, simply driving the chromophore absorption maxima to lower energies is not a good strategy for enhancing r_{33} . All these analyses illustrate the critical role of fine-tuning the electron-donating strength of donor-acceptor polyenes in optimizing their linear and nonlinear optical properties.

The r_{33} values of films containing the four chromophores were measured at different loading densities, as shown in Fig. 8. For chromophores FLD1, the r_{33} values of film-FLD1/APC, were gradually improved from 77 pm/V (10 wt %) to 150 pm/V (25 wt %), while the r_{33} values dropped to 137 pm/V as the loading density increasing from 25 wt % to 30 wt %. The similar trend was also observed for film-FLD2/APC, whose r_{33} values increased from 22 pm/V (10 wt %) to 58 pm/V (25 wt %). The r_{33} values of film-FLD3/APC were improved from 98 pm/V (10 wt %) to 238 pm/V (30 wt %). The similar trend was also observed for film-FLD4/APC whose r_{33} values increased from 29 pm/V (10 wt %) to 82 pm/V (30 wt %). It should be mentioned, the r_{33} values of FLD3/APC are within the highest one ever reported for simple guest host EO polymers when the polymer films doped with chromophores which end-capped with TCF acceptor [1,44,45].

Such a great increase is attributed to the purity and structural features of chromophore FLD3. Its all-trans conformation could provide a better conjugation and increase the $\mu\beta$ value of the chromophores significantly. In addition, the central polyene bridge of chromophore FLD3 is spatially isolated by both the isophorone ring and the center-anchored STBDMS group. This spatial arrangement also greatly increases the solubility of chromophore FLD3 resulting in a higher number density of chromophores that can be incorporated into the polymer matrix. Chromophore FLD3 with a 12-membered ring donor has large three-dimensional steric hindrances, and the STBDMS group also provides effective site isolation to decrease the strong electrostatic interactions among chromophores. When at a low-density range, the intermolecular dipolar interactions are relatively weak. The intermolecular dipole-dipole interactions would become stronger and stronger, accompanying with the increased concentration of NLO chromophore moieties in the polymer which would finally lead to a decreased NLO coefficient. The introduction of side-STBDMS group attached to the conjugated π -bridge can make inter-chromophore electrostatic interactions less favorable, a larger dihedral angle widens the distance between chromophores and weakens the dipole-dipole interactions between dipolar molecules, which benefit the macroscopic electro-optic efficiency [46].

4. Conclusion

A series of highly hyperpolarizable chromophores based on julolidinyl donors with different modified tetraene-derived bridges and CF₃-Ph-TCF or TCF acceptors, has been synthesized and systematically investigated. We compare the structure-property relationship between the 4 s-order chromophores with similar D- π -A structure, but with different position of the functionalized connecting spacer and acceptor. The doped film containing the chromophore FLD1 showed an r_{33} value of 150 pm V⁻¹ at the concentration of 25 wt% at 1.31 μ m. However, the CLD-type chromophores are often a mixture of trans and cis isomers which resulted in reduced $\mu\beta$ value and EO coefficient. We have successfully utilized epoxyisophorone ring-opening chemistry to efficiently incorporate the 2-((tert-butyl(dimethylsilyl)oxy)ethanethiol group to the

bridge of julolidinyl based chromophores FLD3 to ensure its all-trans conformation. The modification of STBDMS group on chromophore can prevent close packing of molecules, and attenuate the strong dipole-dipole electrostatic interactions between chromophores to improve poling efficiency of EO polymers. Compared with the unsubstituted analogue chromophore FLD1, chromophore FLD3 with more isolation groups achieves higher molecular hyperpolarizability and enhanced E-O coefficient. Polymers doped with 30 wt% of a spatially modified chromophore FLD3 have been poled to afford ultra-large electrooptic coefficients (r_{33}) of 238 pm/V. This value is much higher than similar reported NLO chromophore [23,24,47].

Acknowledgments

All calculations were performed on the cluster of Key Laboratory of Theoretical and Computational Photochemistry, Ministry of Education, China. We are grateful to the National Natural Science Foundation of China (No. 21575078, No. 41373118, No. 61101054 and No. 21473227) and Science Foundation of Guangzhou University under Grant No. 27000503171 for the financial support.

References

- [1] Dalton LR, Sullivan PA, Bale DH. Electric field poled organic electro-optic materials: state of the art and future prospects. *Chem Rev* 2010;110(1):25–55.
- [2] Service RF. Nonlinear competition heats up. *Science* 1995;267(5206):1918–21.
- [3] Spiridon MC, Iliopoulos K, Jerca FA, Jerca VV, Vuluga DM, Vasilescu DS, et al. Novel pendant azobenzene/polymer systems for second harmonic generation and optical data storage. *Dyes Pigments* 2015;114:24–32.
- [4] Sullivan PA, Dalton LR. Theory-Inspired development of organic electro-optic materials. *Accounts Chem Res* 2010;43(1):10–8.
- [5] Kityk IV, Sahraoui B, Ledoux-Rak I, Salle M, Migalska-Zalas A, Kazu T, et al. Push-pull chromophores incorporated in 1,3-dithiol-2-ylidene moiety as new electro-optic materials. *Mater. Sci. Eng. B-Solid State Mater. Adv. Technol.* 2001;87(2):148–59.
- [6] Kityk IV, Makowskjanusik M. Optical poling of oligoether acrylate photopolymers doped by stilbene-benzoate derivative chromophores. *J Phys Condens Matter* 2004;16(16):231–40.
- [7] Migalska-Zalas A, Sofiani Z, Sahraoui B, Kityk IV, Tkaczyk S, Yuvshenko V, et al. X-(2) grating in Ru derivative chromophores incorporated within the PMMA polymer matrices. *J Phys Chem B* 2004;108(39):14942–7.
- [8] Sahraoui B, Luc J, Meghea A, Czapllicki R, Fillaut JL, Migalska-Zalas A. Nonlinear optical and surface relief gratings in alkynyl-ruthenium complexes. *J Optic Pure Appl Optic* 2009;11(2).
- [9] El Ouazzani H, Dabos-Seignon S, Gindre D, Iliopoulos K, Todorova M, Bakalska R, et al. Novel styrylquinolinium dye thin films deposited by pulsed laser deposition for nonlinear optical applications. *J Phys Chem C* 2012;116(12):7144–52.
- [10] Zawadzka A, Plociennik P, Strzelecki J, Korcala A, Arof AK, Sahraoui B. Impact of annealing process on stacking orientations and second order nonlinear optical properties of metallophthalocyanine thin films and nanostructures. *Dyes Pigments* 2014;101:212–20.
- [11] Guezguez I, Ayadi A, Ordon K, Iliopoulos K, Branzea DG, Migalska-Zalas A, et al. Zinc induced a dramatic enhancement of the nonlinear optical properties of an azo-based iminopyridine ligand. *J Phys Chem C* 2014;118(14):7545–53.
- [12] Bureš F. Fundamental aspects of property tuning in push-pull molecules. *RSC Adv* 2014;4(102):58826–51.
- [13] Benight SJ, Johnson LE, Knorr DB, Bale DH, Kosilkin I, Olbricht BC, et al. Theory-guided enhancement of poling efficiency of organic electro-optic materials. *Linear and Nonlinear Optics of Organic Materials X* 2010;7774:12.
- [14] Raimundo JM, Blanchard P, Frere P, Mercier N, Ledoux-Rak I, Hierle R, et al. Push-pull chromophores based on 2,2'-bis(3,4-ethylenedioxythiophene) (BEDOT) pi-conjugated spacer. *Tetrahedron Lett* 2001;42(8):1507–10.
- [15] Hammond SR, Clot O, Firestone KA, Bale DH, Lao D, Haller M, et al. Site-isolated electro-optic chromophores based on substituted 2,2'-bis(3,4-propylenedioxythiophene) pi-conjugated bridges. *Chem Mater* 2008;20(10):3425–34.
- [16] Luo JD, Huang S, Cheng YJ, Kim TD, Shi ZW, Zhou XH, et al. Phenyltetraene-based nonlinear optical chromophores with enhanced chemical stability and electrooptic activity. *Org Lett* 2007;9(22):4471–4.
- [17] Liu F, Wang H, Yang Y, Xu H, Zhang M, Zhang A, et al. Nonlinear optical chromophores containing a novel pyrrole-based bridge: optimization of electro-optic activity and thermal stability by modifying the bridge. *J Mater Chem C* 2014;2(37):7785–95.
- [18] He MQ, Leslie TM, Sinicropi JA. alpha-Hydroxy ketone precursors leading to a novel class of electro-optic acceptors. *Chem Mater* 2002;14(5):2393–400.
- [19] Cheng Z, Wang C, Jinglin Yang A, Dalton LR, Sun G, Zhang H, et al. Electric poling and relaxation of thermoset polyurethane second-order nonlinear optical Materials: role of cross-linking and monomer rigidity. *Macromolecules* 2001;34(34):235–43.
- [20] Luo J, Cheng YJ, Kim TD, Hau S, Jang SH, Shi Z, et al. Facile synthesis of highly efficient phenyltetraene-based nonlinear optical chromophores for electrooptics.

- Org Lett 2006;8(7):1387–90.
- [21] Wu J, Liu J, Zhou T, Bo S, Qiu L, Zhen Z, et al. Enhanced electro-optic coefficient (r_{33}) in nonlinear optical chromospheres with novel donor structure. RSC Adv 2012;2(4):1416–23.
- [22] Zhou XH, Luo J, Davies JA, Huang S, Jen AKY. Push-pull tetraene chromophores derived from dialkylaminophenyl, tetrahydroquinolinyl and julolidinyl moieties: optimization of second-order optical nonlinearity by fine-tuning the strength of electron-donating groups. J Mater Chem 2012;22(32):16390–8.
- [23] Zhang C, Dalton LR, Oh MC, Zhang H, Steier WH. Low V- π electrooptic modulators from CLD-1: chromophore design and synthesis, material processing, and characterization. Chem Mater 2001;13(9):3043–50.
- [24] Jin WW, Johnston PV, Elder DL, Manner KT, Garrett KE, Kaminsky W, et al. Structure-function relationship exploration for enhanced thermal stability and electro-optic activity in monolithic organic NLO chromophores. J Mater Chem C 2016;4(15):3119–24.
- [25] Zhang A, Xiao H, Peng C, Bo S, Xu H, Zhang M, et al. Microwave-assisted synthesis of novel julolidinyl-based nonlinear optical chromophores with enhanced electro-optic activity. RSC Adv 2014;4(110):65088–97.
- [26] Cheng Y-J, Luo J, Hau S, Bale DH, Kim T-D, Shi Z, et al. Large electro-optic activity and enhanced thermal stability from diarylaminophenyl-containing high- β nonlinear optical chromophores. Chem Mater 2007;19(5):1154–63.
- [27] Liu F, Xiao H, Yang Y, Wang H, Zhang H, Liu J, et al. The design of nonlinear optical chromophores exhibiting large electro-optic activity and high thermal stability: the role of donor groups. Dyes Pigments 2016;130:138–47.
- [28] Liu F, Wang H, Yang Y, Xu H, Yang D, Bo S, et al. Using phenoxazine and phenothiazine as electron donors for second-order nonlinear optical chromophore: enhanced electro-optic activity. Dyes Pigments 2015;114(0):196–203.
- [29] Bourhill G, Bredas JL, Cheng LT, Marder SR, Meyers F, Perry JW, et al. Experimental demonstration of the dependence of the 1st hyperpolarizability of donor-acceptor-substituted polyenes on the ground-state polarization and bond-length alternation. J Am Chem Soc 1994;116(6):2619–20.
- [30] Zhou X-H, Luo J, Davies JA, Huang S, Jen AKY. Push-pull tetraene chromophores derived from dialkylaminophenyl, tetrahydroquinolinyl and julolidinyl moieties: optimization of second-order optical nonlinearity by fine-tuning the strength of electron-donating groups. J Mater Chem 2012;22(32):16390–8.
- [31] Wuerthner F, Archetti G, Schmidt R, Kuball H-G. Solvent effect on color, band shape, and charge-density distribution for merocyanine dyes close to the cyanine limit. Angew Chem Int Ed 2008;47(24):4529–32.
- [32] Piao X, Zhang X, Inoue S, Yokoyama S, Aoki I, Miki H, et al. Enhancement of electro-optic activity by introduction of a benzyloxy group to conventional donor- π -acceptor molecules. Org Electron 2011;12(6):1093–7.
- [33] Frisch MJ, Trucks GW, Schlegel HB, Scuseria GE, Robb MA, Cheeseman JR, et al. Gaussian 09. Wallingford, CT, USA: Gaussian, Inc.; 2009.
- [34] Liu F, Yang Y, Wang H, Liu J, Hu C, Huo F, et al. Comparative studies on structure–nonlinearity relationships in a series of novel second-order nonlinear optical chromophores with different aromatic amine donors. Dyes Pigments 2015;120:347–56.
- [35] Ma R, Guo P, Yang L, Guo L, Zhang X, Nazeeruddin MK, et al. Theoretical screening of $-NH_2$, $-OH$, $-CH_3$, $-F$, and $-SH$ -substituted porphyrins as sensitizer candidates for dye-sensitized solar cells. J Phys Chem 2010;114(4):1973–9.
- [36] Solomon RV, Veerapandian P, Vedha SA, Venuvanalingam P. Tuning nonlinear optical and optoelectronic properties of vinyl coupled triazene chromophores: a density functional theory and time-dependent density functional theory investigation. J Phys Chem 2012;116(18):4667–77.
- [37] Marder SR, Beratan DN, Cheng LT. Approaches for optimizing the first electronic hyperpolarizability of conjugated organic molecules. Science 1991;252(5002):103–6.
- [38] Kang H, Evmenenko G, Dutta P, Clays K, Song K, Marks TJ. X-shaped electro-optic chromophore with remarkably blue-shifted optical absorption. Synthesis, characterization, linear/nonlinear optical properties, self-assembly, and thin film microstructural characteristics. J Am Chem Soc 2006;128(18):6194–205.
- [39] Park DH, Lee CH, Herman WN. Analysis of multiple reflection effects in reflective measurements of electro-optic coefficients of poled polymers in multilayer structures. Optic Express 2006;14(19):8866–84.
- [40] Dalton LR, Sullivan PA, Bale DH, Bricht BC. Theory-inspired nano-engineering of photonic and electronic materials: noncentro symmetric charge-transfer electro-optic materials. Solid State Electron 2007;51(10):1263–77.
- [41] Wu W, Huang L, Song C, Yu G, Ye C, Liu Y, et al. Novel global-like second-order nonlinear optical dendrimers: convenient synthesis through powerful click chemistry and large NLO effects achieved by using simple azo chromophore. Chem Sci 2012;3(4):1256–61.
- [42] Wu W, Wang C, Li Q, Ye C, Qin J, Li Z. The influence of pentafluorophenyl groups on the nonlinear optical (NLO) performance of high generation dendrons and dendrimers. J Exp Biol 2014;209(8):1454–62.
- [43] Liao Y, Eichinger BE, Firestone KA, Haller M, Luo J, Kaminsky W, et al. Systematic study of the structure-property relationship of a series of ferrocenyl nonlinear optical chromophores. J Am Chem Soc 2005;127(8):2758–66.
- [44] Hammond SR, Clot O, Firestone KA, Bale DH, Lao D, Haller M, et al. Site-isolated electro-optic chromophores based on substituted 2,2'-bis(3,4-propylenedioxythiophene) π -conjugated bridges. Chem Mater 2008;20(10).
- [45] Liu F, Zhang M, Xiao H, Yang Y, Wang H, Liu J, et al. Auxiliary donor for tetrahydroquinoline-containing nonlinear optical chromophores: enhanced electro-optical activity and thermal stability. J Mater Chem C 2015;3(36):9283–91.
- [46] Huang HY, Deng GW, Liu JL, Wu JY, Si P, Xu HJ, et al. A nunchaku-like nonlinear optical chromophore for improved temporal stability of guest-host electro-optic materials. Dyes Pigments 2013;99(3):753–8.
- [47] Zhou XH, Davies J, Huang S, Luo J, Shi Z, Polishak B, et al. Facile structure and property tuning through alteration of ring structures in conformationally locked phenyltetraene nonlinear optical chromophores. J Mater Chem 2011;21(12):4437–44.